

150 to 200 m (5). It was probably a nekto-benthic scavenger and predator, like most Recent myodocopes. The long natatory setae and large basipod of the second antenna imply that it was an adept swimmer. Its apparently limited dispersal capacity [one locality, even though myodocope ostracodes of the Welsh sedimentary basin have been extensively studied (16, 17)] indicates that it had a benthic rather than pelagic lifestyle. The endites on appendages 3 to 5 seem suitable for comminuting food. As in Recent myodocopids (18, 19), the well-developed furca may have been used to hold and cut prey and carrion, and the processes on the labrum may have secreted enzymes to aid digestion and substances for food entanglement and bioluminescence.

C. eplecticos proffers unequivocal evidence for the occurrence of Ostracoda in the Paleozoic. It also allows for a particular sex to be identified in an animal as old as Silurian (hemipenes occur in the Cretaceous species). Its morphological similarity to Recent myodocopids (the only notable soft part difference from living cylindroleberidids is its apparent lack of a setose comb on the fifth appendage) demonstrates evolutionary stasis within the group over 425 million years and echoes the low rates of change that are known in other crustaceans (20). The find also accords with molecular evidence (14) suggesting that cylindroleberidids originated in the Early Paleozoic.

C. eplecticos has the only known undoubted gills in a fossil ostracode and provides the earliest direct evidence of a respiratory-cum-circulatory system in the group: The epipod on the second maxilla presumably functioned to ventilate the domiciliar cavity, and the gills with thickened edges (the site of hypobranchial and epibranchial canals in Recent cylindroleberidids) (21) indicate the presence of branchial circulation and, therefore, an integrated vascular circulatory system with a heart.

References and Notes

1. D. J. Horne, A. Cohen, K. Martens, *Geophys. Monogr.* **131**, 5 (2002).
2. X.-G. Hou, D. J. Siveter, M. Williams, D. Walossek, J. Bergström, *Philos. Trans. R. Soc. London Ser. B* **351**, 1131 (1996).
3. R. J. Smith, *Palaeontology* **43**, 63 (2000).
4. K. J. Müller, in *Proceedings of the 7th International Symposium on Ostracods*, N. Krstic, Ed. (Serbian Geological Society, Belgrade, Yugoslavia, 1979), pp. 5–9.
5. D. E. G. Briggs, David J. Siveter, Derek J. Siveter, *Nature* **382**, 248 (1996).
6. P. J. Orr, D. E. G. Briggs, David J. Siveter, Derek J. Siveter, *J. Geol. Soc. London* **157**, 173 (2000).
7. M. D. Sutton, D. E. G. Briggs, David J. Siveter, Derek J. Siveter, *Nature* **410**, 461 (2001).
8. M. D. Sutton, D. E. G. Briggs, David J. Siveter, Derek J. Siveter, *Proc. R. Soc. London Ser. B* **268**, 2355 (2001).
9. M. D. Sutton, D. E. G. Briggs, David J. Siveter, Derek J. Siveter, *Paleontol. Electronica* **4**, article 2 (2001) (http://palaeo-electronica.org/2001_1/s2/issue1_01.htm).
10. M. D. Sutton, D. E. G. Briggs, David J. Siveter, Derek J.

- Siveter, P. J. Orr, *Proc. R. Soc. London Ser. B* **269**, 1195 (2002).
11. A. R. Parker, *J. Mar. Biol. Assoc. U. K.* **77**, 1223 (1997).
12. D. J. Siveter, J. M. C. Vannier, *Trans. R. Soc. Edinb. Earth Sci.* **81**, 45 (1990).
13. S. E. Gabbott, D. J. Siveter, R. J. Aldridge, J. N. Theron, *Lethaia*, **36**, 151 (2003).
14. S. Yamaguchi, K. Endo, *Mar. Biol.* **143**, 23 (2003).
15. L. S. Kornicker, *Smithson. Contrib. Zool.* **319**, 1548 (1981).
16. D. J. Siveter, *Natl. Mus. Wales Geol. Ser.* **9**, 252 (1989).
17. D. J. Siveter, J. M. C. Vannier, D. C. Palmer, *J. Micro-palaeontol.* **10**, 151 (1991).
18. A. R. Parker, *J. Crustac. Biol.* **17**, 632 (1997).

19. J. Vannier, K. Abe, K. Ikuta, *Mar. Biol.* **132**, 391 (1998).
20. D. Walossek, *Fossils Strata* **32**, 1–202 (1993).
21. J. Vannier, K. Abe, K. Ikuta, *J. Crustac. Biol.* **16**, 453 (1996).
22. S. Hiruta, *J. Fac. Sci. Hokkaido Univ.* **22**, 9 (1979).
23. We thank the Leverhulme Trust (grant F/08581/E) and the Natural Environment Research Council (grant GR3/12053) for their support (both grants to Derek J.S., D.E.G.B., and David J.S.); R. Smith, G. Boxshall, and S. Hiruta for access to Recent material; T. Hall, J. Sinclair, and A. Swift for general assistance; two anonymous referees; and the University of Leicester (David J.S.; study leave).

10 September 2003; accepted 16 October 2003

Regulation of Flowering Time by Histone Acetylation in *Arabidopsis*

Yuehui He, Scott D. Michaels, Richard M. Amasino*

The *Arabidopsis* autonomous floral-promotion pathway promotes flowering independently of the photoperiod and vernalization pathways by repressing *FLOWERING LOCUS C (FLC)*, a MADS-box transcription factor that blocks the transition from vegetative to reproductive development. Here, we report that *FLOWERING LOCUS D (FLD)*, one of six genes in the autonomous pathway, encodes a plant homolog of a protein found in histone deacetylase complexes in mammals. Lesions in *FLD* result in hyperacetylation of histones in *FLC* chromatin, up-regulation of *FLC* expression, and extremely delayed flowering. Thus, the autonomous pathway regulates flowering in part by histone deacetylation. However, not all autonomous-pathway mutants exhibit *FLC* hyperacetylation, indicating that multiple means exist by which this pathway represses *FLC* expression.

The developmental transition from a vegetative to a reproductive phase in *Arabidopsis* is genetically controlled by several pathways, which integrate the endogenous developmental state of the plant and environmental cues (1). The autonomous and the vernalization pathways independently regulate the floral transition by repressing *FLC* expression (2–4). There are six genes in the autonomous pathway: *FLD*, *FCA*, *FPA*, *FY*, *FVE*, and *LUMINIDEPENDENS (LD)* (1, 2). *FCA* and *FPA* encode RNA binding proteins (5, 6), *FY* encodes a protein involved in mRNA 3' processing (7), and *LD* encodes a homeodomain-containing protein (8).

We have previously identified *FLD* as an autonomous-pathway gene by an analysis of *fld-1* (9). The *fld-1* mutant, which is in the Columbia (Col) accession, was crossed with the Landsberg *erecta* accession to create a segregating population for the map-based cloning of *FLD* (fig. S1). *FLD* consists of two exons (Fig. 1A) that encode a protein of 789 amino acid residues (*FLD* is locus At3g10390, see www.arabidopsis.org). The *fld-1* lesion is a point

mutation (C to T) that converts Arg¹⁰ (CGA) into a premature stop codon (TGA). After the identification of *FLD*, two additional *fld* mutants (*fld-3* and *fld-4*) were obtained from the Salk Institute Genome Analysis Laboratory collection (10). Both alleles are the result of transferred DNA (T-DNA) insertions in the coding region (Fig. 1A), and neither expresses the full-length *FLD* mRNA (Fig. 1B).

All of the *fld* mutants flowered much later than wild-type Col in inductive long-day photoperiods (Table 1 and Fig. 2A) and flowered rapidly after exposure to a prolonged period of cold (vernalization) (Table 1), which is characteristic of autonomous-pathway mutants (2). The two T-DNA mutants flowered later than *fld-1* (Table 1); thus, although the *fld-1* lesion is a premature stop codon, this allele may have residual activity. *fld-3* and *fld-4* mutants flower later than any other autonomous mutant in the Col genetic background (Table 1) (11), and extensive aerial rosettes, which are often associated with extremely delayed flowering, are produced at the early nodes of the main inflorescence stem (Fig. 2, A and B).

Steady-state *FLC* mRNA levels are much higher in the *fld* mutants than in the parental Col line (Fig. 2D). Increased *FLC* expression is characteristic of other autonomous mutants

Department of Biochemistry, University of Wisconsin, Madison, WI 53706, USA.

*To whom correspondence should be addressed. E-mail: amasino@biochem.wisc.edu

REPORTS

such as *fca* and *fve*, and lines containing *FRIGIDA* (*FRI*), which is an activator of *FLC* that confers the vernalization-responsive late-flowering habit in many winter-annual accessions of *Arabidopsis* (12) (Fig. 2D). In addition, the late-flowering phenotype of *fld* is completely suppressed by the loss of *FLC*; the *fld-1 fld-3* double mutant flowers like *fld-3* in long days (Table 1 and Fig. 2C). Thus, the role of *FLD* in flowering-time control is to repress *FLC* expression.

To examine the *FLC* spatial expression pattern in *fld* mutants, a translational *FLC::GUS* fusion (13) was introduced into *fld-3*. *FLC* was preferentially expressed in shoot and root apical regions, which are enriched in dividing cells (Fig. 2E). This *FLC* expression pattern is identical to that of *FLC::GUS* in a *FRI*-containing line (Fig. 2E). Thus, an *fld* lesion causes *FLC* expression to increase in the same spatial pattern as that caused by *FRI* in winter annuals. As might be expected for a regulator of *FLC*, the pattern of *FLD* expression is identical to that of *FLC*, as determined by a translational *FLD::GUS* fusion (Fig. 2F) (13) and by reverse transcription polymerase chain reaction analyses of the native mRNAs (11).

FLD is a plant homolog of the human protein KIAA0601 (14); *FLD* is 42% identical to KIAA0601 over a region of 568 amino acids, and the similarity between these two proteins over the same region is about 60% (fig. S2). Much of *FLD* and KIAA0601 (14) consist of a region that is similar to human polyamine oxidase 1 (HsPAO1) (15), maize polyamine oxidase (ZmPAO) (16), and a predicted *Arabidopsis* polyamine oxidase (AtPAO, At5g13700; see www.arabidopsis.org) (Fig. 3A and fig. S2). Crystal structure-derived residues of ZmPAO that are involved in binding the cofactor FAD (16) are conserved in all five proteins (fig. S2). However, *FLD* and KIAA0601 contain an additional region—recently referred to as a SWI3p, Rsc8p, and Moira (SWIRM) domain (17)—in the N-terminal region (Fig. 3A and

fig. S2). SWIRM domains are found in a range of proteins involved in chromatin remodeling (17). The joining of a SWIRM domain to a polyamine oxidase is found in *FLD*, two related genes in *Arabidopsis* (At1g62830 and At3g13682, see www.arabidopsis.org), and three related genes in rice (fig. S3) (11). In human, mouse, and *Drosophila*, only one such gene in each has been identified to date (*KIAA0601*, *LOC230843*, and *CG17149*, respectively) (fig. S3), and two have been identified in *Caenorhabditis elegans* (18) (fig. S3).

The human protein KIAA0601 is a component of human histone deacetylase 1,2 (HDAC1/2) co-repressor complexes (14, 19). These complexes are involved in initiating repression of gene expression by deacetylation of histone residues (19). However, whether KIAA0601 is required for the deacetylation activity of this complex is not known. To explore whether *FLD* has a role in deacetylation, we examined the acetylation

state of histone H4 at the *FLD* target, *FLC*, by chromatin immunoprecipitation (ChIP) (13). Compared with acetylation of *FLC* chromatin in the wild-type plant, H4 in *fld* is hyperacetylated (Fig. 3B). The hyperacetylation occurs in the region close to the transcription initiation point, the first intron, and in a region of the second intron (fig. S4). The acetylation difference is not detectable in a region about 2 kb 5' to the translation initiation point or in a region of the last exon (fig. S4C). Thus, *FLC* hyperacetylation in *fld* occurs in a defined region similar to that reported for another plant gene (20).

In contrast to the situation in *fld*, there is no change in *FLC* acetylation in several other mutants of autonomous-pathway genes (*fca*, *fpa*, and *ld*) or in a *FRI*-containing line (Fig. 3B and fig. S4). However, like *fld*, the autonomous-pathway mutant *fve* exhibits an increase in *FLC* acetylation, although this increase is not as large as that in *fld* (Fig. 3B).

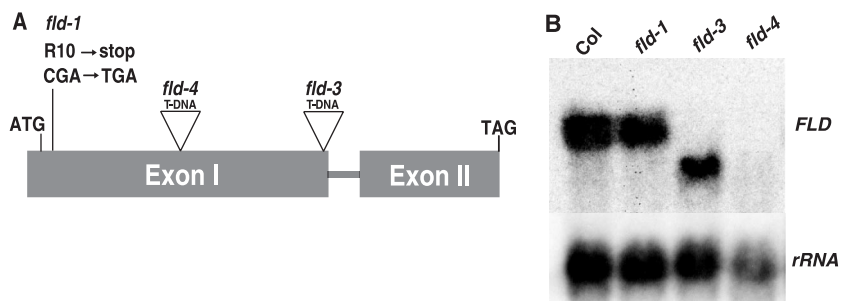


Fig. 1. Structure and expression of *FLD*. (A) *FLD* gene structure. Triangles indicate T-DNA insertions; the T-DNA was located 1.6 kb downstream of the translational initiation codon in *fld-3* and 0.8 kb downstream of the initiation codon in *fld-4*. (B) *FLD* mRNA accumulation in seedlings determined by RNA blot analysis. About 20 μ g of total RNA extracted from 10-day-old seedlings was loaded in each lane. R10, Arg¹⁰; stop, stop codon.

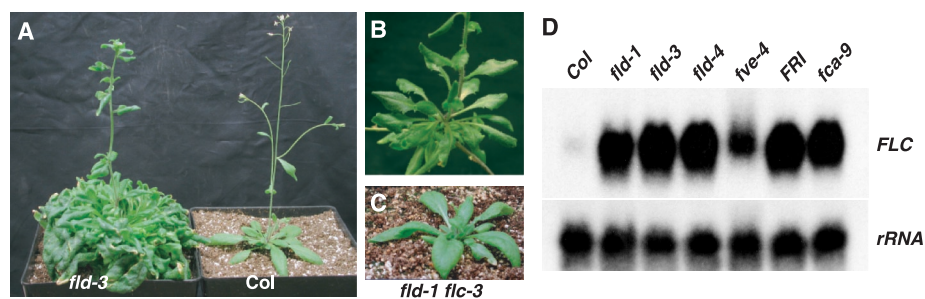


Fig. 2. Phenotype of *fld* mutants. (A) *fld* mutants flower later than wild-type plants in long days. (B) A single node on the main inflorescence stem of *fld-3* showing an aerial rosette. (C) *FLC* dependence of *fld* phenotype. The *fld-1 fld-3* double mutant flowers early like *fld-3*. (D) Abundance of *FLC* mRNA in *fld*, *fve*, *fca*, and *FRI*^{Sf2}-Col [FRI^{Sf2}-Col is a line in which a functional *FRI* allele from the San Felu-2 (Sf-2) accession was introgressed into the Col background (3)]. About 20 μ g of total RNA extracted from 10-day-old seedlings was loaded in each lane, and the blot was hybridized first with a *FLC* probe and subsequently with an 18S *rDNA* probe. (E) *FLC::GUS* transgene expression pattern in Col, *fld-3*, and *FRI* backgrounds. Arrowheads indicate stained tissues. Scale bars, 1 mm. (F) *FLD::GUS* (translation fusion) expression pattern in *fld-1*. Scale bar, 1 mm.

Table 1. Flowering times of plants in the long-day condition. Values shown are mean numbers \pm SD. Numbers in parentheses are the total numbers of plants evaluated. vern, 44-day vernalization.

Line	Rosette leaf number	Node number*
Col	12.7 \pm 1.2 (9)	2.9 \pm 0.8
<i>fld-1</i>	60.4 \pm 14.2 (8)	8.5 \pm 0.6
<i>fld-1</i> + vern	14.8 \pm 1.7 (12)	3.9 \pm 0.5
<i>fld-3</i>	93.5 \pm 21.8 (19)	12.5 \pm 4.6
<i>fld-3</i> + vern	17.1 \pm 1.1 (13)	5.5 \pm 0.7
<i>fld-4</i>	86.0 \pm 18.0 (20)	12.2 \pm 0.9
FRI ^{Sf2} -Col	78.2 \pm 8.8 (7)	10.8 \pm 0.8
FRI ^{Sf2} -Col + vern	15.9 \pm 1.3 (7)	4.4 \pm 1.3
<i>fve-4</i>	40.8 \pm 3.7 (6)	6.5 \pm 1.0
<i>fld-1 fld-3</i>	12.1 \pm 0.7 (7)	2.7 \pm 0.9
<i>fld-3</i>	10.2 \pm 1.1 (9)	2.1 \pm 0.6

*Total node number of the main inflorescence stem.

Consistent with the weaker hyperacetylation phenotype of *five-4* compared with *fld*, *five-4* is also not as delayed in flowering as are the *fld* mutants (Table 1). The weaker flowering and acetylation phenotypes of *five* might result from redundancy of *FVE* function in the *Arabidopsis* genome or partial activity of *five-4* allele. These data indicate that both FLD and *FVE* are involved in *FLC* repression by histone deacetylation, perhaps as components of a HDAC co-repressor complex.

The *FLC* hyperacetylation phenotype of *fld* indicates that FLD is required for the ability of certain HDACs to regulate *FLC*. The *Arabidopsis* genome contains four homologs of human *HDAC1/2* (*AtHDA1*, *AtHDA6*, *AtHDA7*, and *AtHDA9*; see www.chromdb.org). However, *AtHDA* mutants that have a phenotype similar to *fld* have not been

found. Thus, either the HDAC that participates in *FLC* regulation with FLD is also involved in other processes and a mutation in it is highly pleiotropic or lethal, or there is redundancy among the *Arabidopsis HDACs* such that no single mutant will have a large effect on flowering time. Suppression of *AtHDAs* by an antisense construct that is likely to have partially suppressed the expression of several *HDACs* does cause delayed flowering (21).

HDAC complexes are typically recruited to target genes through an interaction with cis-regulatory DNA elements. For example, the KIAA0601-CoREST HDAC1/2 co-repressor complex represses neuron-specific genes in nonneuronal cells by means of the cis-regulatory element known as repressor element 1 (22). To determine whether a spe-

cific region of the *FLC* locus is required for histone deacetylation, we created a series of internal deletions in the region 5' of the translation start codon and the first intron of *FLC* because *FLC* expression is regulated by these regions (23) (Fig. 4A), and we introduced these constructs into the *fld-3* null mutant in the Col background. Deletion of a region required for *FLC* deacetylation might produce a phenocopy of the *fld* mutant. Indeed, deletion of a 295-base pair region of Intron I caused extremely late flowering in transgenic plants (Fig. 4, B and C), and in these transgenic lines, this *FLC* transgene was both highly expressed (Fig. 4D) and hyperacetylated (Fig. 4E). Deletions in other regions of *FLC* did not cause hyperacetylation of *FLC* transgenes (Fig. 4E) or an extreme delay of flowering (11). Thus, a specific region in the first intron of *FLC* is required for deacetylation.

The modification of the level of acetylation in *FLC* chromatin suggests a mechanism by which certain autonomous-pathway genes regulate *FLC* expression. The autonomous pathway was originally defined as a set of genes with a specific mutant phenotype: vernalization and photoperiod-responsive late flowering (24). Genetic analyses indicate that the autonomous pathway may in fact be composed of genes that control flowering by more than one mechanism (25). Our observation that hyperacetylation of *FLC* chromatin is only observed in *fld* and *five* mutants supports a model in which FLD and *FVE* regulate *FLC* expression by a mechanism distinct from other autonomous-pathway genes. Given the centrality of *FLC* in flowering-time control, it is not surprising that *FLC* is subject to multiple independent regulators.

Fig. 3. Domain architecture of FLD and acetylation of *FLC* chromatin. (A) Domain architectures of FLD and related proteins. FLD and Hs-KIAA0601 consist of a SWIRM domain joined to a region similar to maize and human polyamine oxidases (ZmPAO and HsPAO1). GenBank accession numbers: NM_111874, AtFLD; BC048134, Hs-KIAA0601; CAA05249, ZmPAO; AAK55763, HsPAO1. (B) ChIP analyses of the acetylation state of histone H4 in *FLC* chromatin. The input is Col chromatin before immunoprecipitation. No AB, control sample lacking antibody; *co*, a late-flowering mutant in the photoperiod pathway, in which *FLC* expression level is not changed (26), that served as a control. *ACTIN* served as an internal control of the ChIP analysis. The fold enrichment of a mutant compared to Col was calculated as follows: *FLC* and *ACTIN* in the mutant sample were first normalized to *FLC* and *ACTIN* in the Col sample; the normalized *FLC* was then divided by the normalized *ACTIN* to obtain the fold enrichment in the mutant. The fold enrichment of mutants over Col is shown.

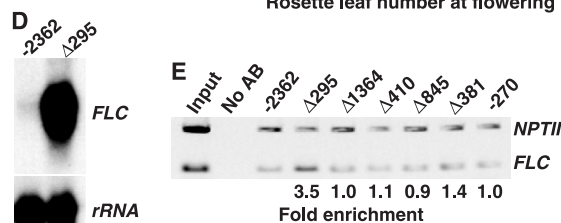
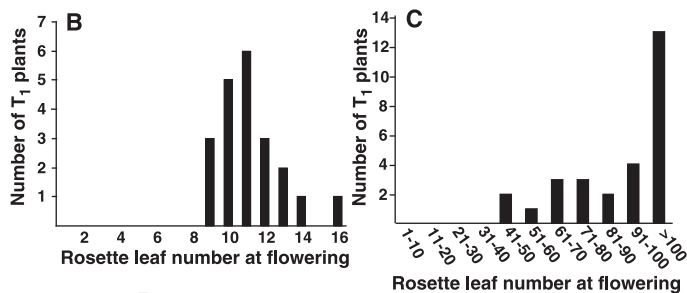
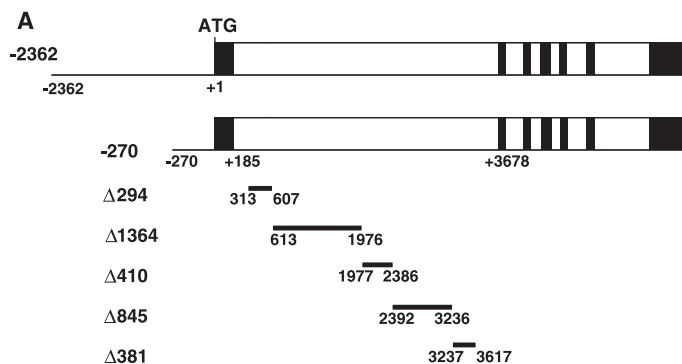
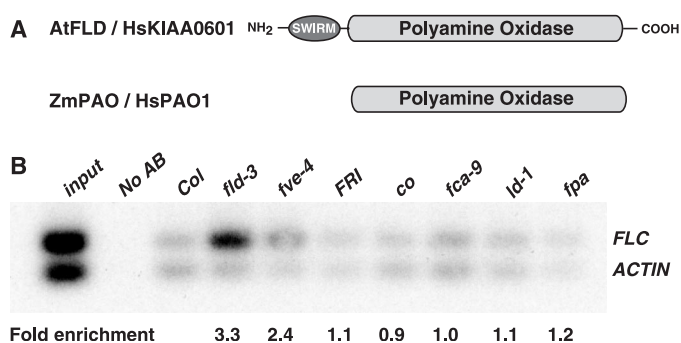


Fig. 4. Deletion of a region ($\Delta 295$) in the first intron of *FLC* phenocopies the *fld* phenotype. (A) Internal deletions in the *FLC* genomic region. The translation initiation point is +1. The filled boxes represent exons, and the open boxes represent introns. (B) Flowering times of first transformed generation (T_1) transgenic plants derived from construct -2362 (a fully functional *FLC* transgene). (C) Flowering times of T_1 transgenic plants derived from intron deletion $\Delta 295$. (D) Abundance of *FLC* mRNA in T_1 transgenic plants derived from the construct -2362 and the $\Delta 295$ deletion. (E) ChIP analyses of the acetylation state of histone H4 in *FLC* transgene chromatin. The input is the chromatin of *fld-3* transformed with construct -2362 before immunoprecipitation. No AB, control sample lacking antibody. The transformant selection marker gene *NPTII* served as an internal control for the ChIP analyses. The fold enrichment (calculated as described in Fig. 3B legend) of the deletions compared with the -2362 construct is shown.

References and Notes

1. A. Mouradov, F. Cremer, G. Coupland, *Plant Cell* **14**, S111 (2002).
2. G. G. Simpson, A. R. Gendall, C. Dean, *Annu. Rev. Cell Dev. Biol.* **15**, 519 (1999).
3. S. D. Michaels, R. M. Amasino, *Plant Cell* **11**, 949 (1999).
4. C. C. Sheldon *et al.*, *Plant Cell* **11**, 445 (1999).
5. R. Macknight *et al.*, *Cell* **89**, 737 (1997).
6. F. M. Schomburg, D. A. Patton, D. W. Meinke, R. M. Amasino, *Plant Cell* **13**, 1427 (2001).
7. G. G. Simpson, P. P. Dijkwel, V. Quesada, I. Henderson, C. Dean, *Cell* **113**, 777 (2003).
8. I. Lee *et al.*, *Plant Cell* **6**, 75 (1994).
9. S. L. Sanda, R. M. Amasino, *Plant Physiol.* **111**, 641 (1996).
10. J. M. Alonso *et al.*, *Science* **301**, 653 (2003).
11. Y. He, R. M. Amasino, data not shown.
12. U. Johanson *et al.*, *Science* **290**, 344 (2000).
13. Materials and methods are available as supporting material on Science Online.
14. G. W. Humphrey *et al.*, *J. Biol. Chem.* **276**, 6817 (2001).
15. T. Murray-Stewart, Y. Wang, W. Devereux, R. A. Casero Jr., *Biochem. J.* **368**, 673 (2002).
16. C. Binda *et al.*, *Structure* **7**, 265 (1999).
17. L. Aravind, L. M. Iyer, *Genome Biol.* **3**, RESEARCH0039.1 (2002).
18. S. Eimer, B. Lakowski, R. Donhauser, R. Baumeister, *EMBO J.* **21**, 5787 (2002).
19. M. A. Hakimi, Y. Dong, W. S. Lane, D. W. Speicher, R. Shiekhhattar, *J. Biol. Chem.* **278**, 7234 (2003).
20. Y. L. Chua, L. A. Watson, J. C. Gray, *Plant Cell* **15**, 1468 (2003).
21. L. Tian, Z. J. Chen, *Proc. Natl. Acad. Sci. U.S.A.* **98**, 200 (2001).
22. M. A. Hakimi *et al.*, *Proc. Natl. Acad. Sci. U.S.A.* **99**, 7420 (2002).
23. C. C. Sheldon, A. B. Conn, E. S. Dennis, W. J. Peacock, *Plant Cell* **14**, 2527 (2002).
24. M. Koornneef, C. J. Hanhart, J. H. van der Veen, *Mol. Gen. Genet.* **229**, 57 (1991).
25. M. Koornneef, C. Alonso-Blanco, H. Blankestijn-de Vries, C. J. Hanhart, A. J. Peeters, *Genetics* **148**, 885 (1998).
26. A. Samach *et al.*, *Science* **288**, 1613 (2000).
27. We thank S. Sanda for the initial characterization of *fld-1* and for creating segregating populations that

were used in map-based cloning; S. Sung for insightful discussions; M. R. Doyle for critical reading of this paper; J. M. Martinez-Zapater for providing the *five* allele in the Col background; and the Salk Institute Genome Analysis Laboratory and the Arabidopsis Biological Resource Center at Ohio State for providing T-DNA insertion pools containing alleles of *fld-3* and *fld-4*. Supported by the College of Agricultural and Life Sciences and the Graduate School of the University of Wisconsin, the U.S. Department of Agriculture National Research Initiative Competitive Grants Program, and NSF grant 0133663 to R.M.A.

Supporting Online Material

www.sciencemag.org/cgi/content/full/1091109/DC1
Materials and Methods

Figs. S1 to S4

References

3 September 2003; accepted 15 October 2003

Published online 30 October 2003;

10.1126/science.1091109

Include this information when citing this paper.

Ecological Adaptation During Incipient Speciation Revealed by Precise Gene Replacement

Anthony J. Greenberg,¹ Jennifer R. Moran,² Jerry A. Coyne,^{1,2} Chung-I Wu^{1,2,*}

To understand the role of adaptation in speciation, one must characterize the ecologically relevant phenotypic effects of naturally occurring alleles at loci potentially causing reproductive isolation. The *desaturase2* gene of *Drosophila melanogaster* is such a locus. Two geographically differentiated *ds2* alleles underlie a pheromonal difference between the Zimbabwe and Cosmopolitan races. We used a site-directed gene replacement technique to introduce an allele of *ds2* from the Zimbabwe population into Cosmopolitan flies. We show that the Cosmopolitan allele confers resistance to cold as well as susceptibility to starvation when the entire genetic background is otherwise identical. We conclude that ecological adaptation likely accompanies sexual isolation between the two behavioral races of *D. melanogaster*.

It is often suggested that adaptation is the driving force behind divergence of populations leading to speciation (1–3). Population genetic and ecological data appear to support this view (1, 3). However, establishing a causal link between a mutation, its effect on differential adaptation, and its effect, if any, on reproductive isolation has been difficult. A molecular genetic approach to this problem can be successful only if one is able to exchange naturally occurring alleles of candidate isolation genes between incipient species. Most important, the changes must involve only the gene under consideration, leaving the rest of the genome intact.

We focused on a naturally occurring DNA sequence polymorphism at the *desaturase2*

(*ds2*) locus of *Drosophila melanogaster*. This locus encodes a Δ^9 fatty acid desaturase identified by mapping and association as the gene responsible for a cuticular hydrocarbon (CH) polymorphism between populations of this species (4–6). Hydrocarbons are mating pheromones in many insects (7, 8), and differences in CH composition contribute to reproductive isolation between some *Drosophila* species (9, 10). The functional *ds2^Z* allele is found at high frequency in African and Caribbean populations. Females from these populations produce 5,9-heptacosadiene (5,9-HD) as the predominant CH. A 16-bp (base pair) deletion 5' of *ds2* (*ds2^M*) results in apparent inactivation of the *ds2* gene (5, 6). As a result, cuticles of Cosmopolitan females are rich in 7,11-heptacosadiene (7,11-HD) instead of 5,9-HD. The loss-of-function *ds2^M* allele has spread throughout the rest of the world. Patterns of nucleotide diversity at the locus suggest that this spread may have occurred under the influence of positive selection (6).

In addition to its role in CH polymorphism, *ds2* is one of the candidate genes potentially responsible for strong premating isolation between females from Zimbabwe (Z) and males from Cosmopolitan (M) populations (11). These recently diverged populations may be incipient species (12–14). Whether *ds2* influences sexual isolation or not, the marked geographic pattern of *ds2* allele distribution has to be explained. We wanted to know whether some ecological forces are involved in the maintenance of this polymorphism and, if so, what those forces may be. Are different *ds2* alleles perhaps favored in different environments?

We can begin answering these questions by comparing the phenotypic and fitness effects of *ds2^M* and *ds2^Z* in a constant genetic background. However, conventional transgene technology, even in *D. melanogaster*, one of the most experimentally tractable model organisms, is not sufficient for the task. This approach does not allow targeting of the endogenous locus, and integration occurs at unpredictable sites in the genome. The influence of the surrounding chromosome environment on the expression of the transgene, as well as the effect of the insertion event itself on the neighboring genes, can yield a large variance in the expression of the trait being studied. This variability can greatly reduce, or even eliminate, the power to detect subtle differences in phenotype that are frequently of great importance in nature (15). The alternative approach based on backcross and introgression [e.g., (16, 17)] does not offer the requisite control of genetic background.

Recent development of gene disruption in *D. melanogaster* by Rong and Golic (18, 19) makes it possible to precisely manipulate any gene at its locus, thus eliminating most of the difficulties described above. We applied this technique in an attempt to shed light on the

¹Department of Ecology and Evolution, ²Committee on Genetics, The University of Chicago, Chicago, IL 60637, USA.

*To whom correspondence should be addressed. E-mail: ciwu@uchicago.edu